LINKS BETWEEN ERUPTIVE STYLES, MAGMATIC EVOLUTION, AND MORPHOLOGY OF SHIELD VOLCANOES: SNAKE RIVER PLAIN, IDAHO

Katelyn J. Barton, Eric H. Christiansen, and Michelle Hurst
Department of Geological Sciences, Brigham Young University, Provo, Utah

Abstract

Despite their similar ages and geographic locations, two low-shield volcanoes on the eastern Snake River Plain, Idaho, Kimama Butte (87 ka) and Rocky Butte (95 ka), have strikingly different profiles. In this study, these two volcanoes are examined to determine the connections between chemical composition, intensive parameters, eruption style, and topographic features of basaltic shield volcanoes. Because lava temperature, magma viscosity, and chemical composition overlap at the two volcanoes, they are probably not important controls on the differences in morphology. The main difference at the two shields, aside from general vent morphology, is the presence of late-stage, phenocryst-rich, high viscosity lavas that form high spatter ramparts at Kimama Butte but not at Rocky Butte. We conclude that phenocryst abundance, magma viscosity, and eruption style play the most important role in developing a shield volcano summit. Where eruptions shifted from lava lake overflow and tube development to late fountaining with short, viscous, spatter-fed, phenocryst-rich flows, a steeper, higher shield developed. The result can be used to better understand the eruptive processes of shield volcanoes on the Moon, Mars, and Venus that can only be studied morphologically.

INTRODUCTION

Limitations due to physical distance from other planetary bodies makes understanding the volcanic systems on them difficult. Estimations of the chemical composition of lavas is especially challenging and often constrained based on morphology (Guest et al., 1992; Sakimoto et al., 2003). To overcome these difficulties, it is beneficial to study similar terrains on Earth where our access is less limited. In particular, since volcano morphology is a parameter that can be accurately assessed with the techniques currently used in planetary exploration, it is important to understand the morphology of similar terrestrial shield volcanoes.

The eastern Snake River Plain, Idaho is one such terrain that is analogous to volcanic provinces on the Moon, Mars, and Venus (e.g. Greeley and Spudis, 1981; Head and Gifford, 1980; Guest et al., 1992; Hughes, 2001; Sakimoto et al., 2003; Hughes et al., 2004; Hauber et al., 2009; Henderson, 2015; Hughes et al., 2019). Three categories of morphological profiles, 'capped', low-profile, or dome-shaped, are present on the Snake River Plain (Sakimoto et al., 2003; Hughes et al., 2004). The low-profile shield summit regions are slightly elevated compared to the rest of the shield while the 'capped' variety have markedly steeper flanks near the vent and a distinct elevated cap at the summit (Hughes et al., 2004).

Kimama Butte and Rocky Butte represent the range of morphologies typical of shield volcanoes on the eastern Snake River Plain (Fig. 1). Kimama Butte, a 'capped' shield variety, has a diameter of 9 km and a height of 210 m with only a small central crater at the main vent. In contrast, Rocky Butte is a low-profile shield with a broad 12 km topographic shield that rises 140 m to the summit with less than 1-degree slopes. The summit is marked by a shallow, slightly elongated crater.

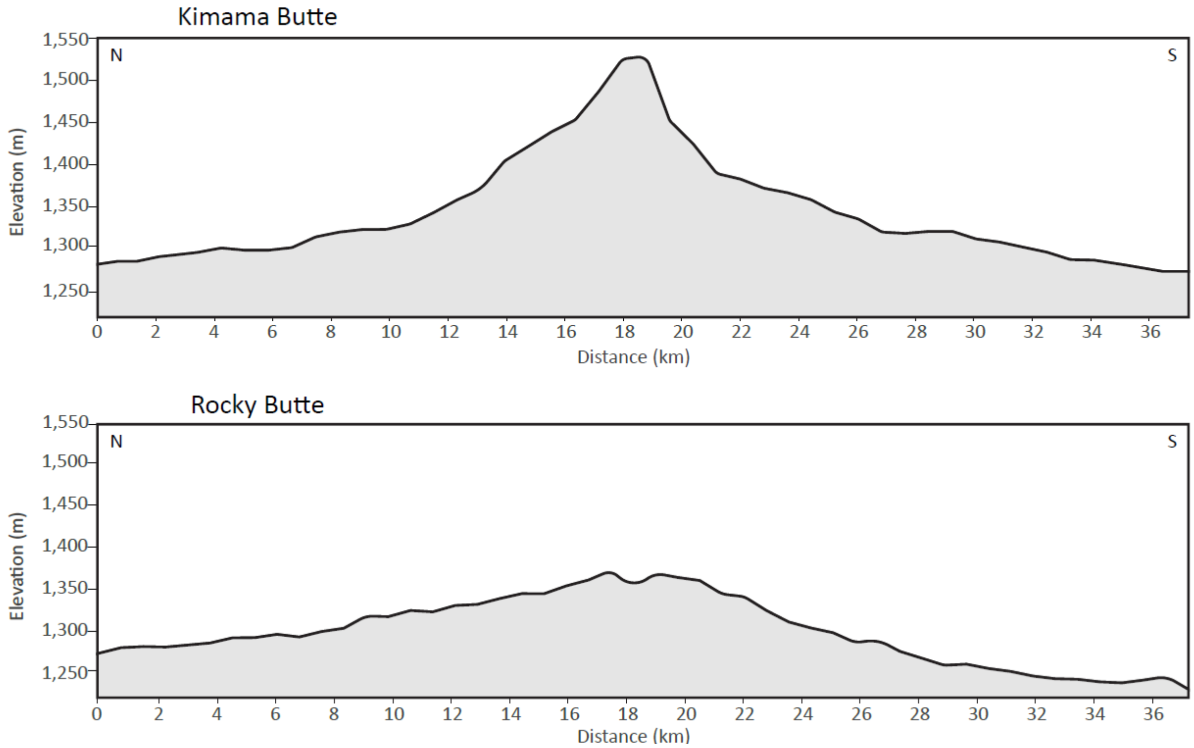

Figure 1. North-south profiles of Kimama Butte and Rocky Butte. Notice Rocky Butte is a low-profile shield while Kimama Butte has a steep 'cap' near the summit. 15:1 vertical exaggeration.

The main purpose of this study is to determine the connection between chemical compositions, eruption styles, and topographic features of basaltic shield volcanoes. In particular, we will test the assertions of previous studies that have linked more evolved chemical compositions (Hughes and Sakimoto, 2002; Sakimoto et al., 2003), changes in eruptive style (Hughes and Sakimoto, 2002; Brady, 2005), and lavas with higher crystallinity (Brady, 2005) with the steeper portions of shields. If such interrelationships can be understood on Earth with these two low-shield volcanoes, information can be unlocked about the many other shield volcanoes in the solar system.

GEOLOGIC SETTING

Kimama Butte and Rocky Butte are two of approximately 300 low-shield volcanoes (Henderson, 2015) scattered along the 400 km long, 100 km wide eastern Snake River Plain that trends east-northeast across southern Idaho to the edge of Yellowstone Plateau volcanic field. Characteristic of the area is an extensive record of bimodal volcanism (basalt and rhyolite) with few intermediate compositions (Hughes et al., 1999; Christiansen and McCurry, 2008; Colón et al., 2018). The time-transgressive Miocene-Quaternary rhyolites are associated with the Yellowstone hot spot track (Hughes et al., 1999). Covering the rhyolitic calderas and volcanic centers are younger basaltic lavas and sediments from eolian, fluvial, and lacustrine processes (Hughes et al., 2002).

A deep-mantle plume is the most widely accepted explanation for this mid-plate volcanism (Leeman, 1982; Pierce et al., 1992; McQuarrie and Rodgers, 1998; Perfit and Davidson, 2000; Hughes et al., 2002; Colón et al., 2018); however, other mechanisms such as an upper-mantle plume or decompression melting from extension of a rift in the lithosphere are still maintained (Christiansen et al., 2002; Foulger et al., 2015). Decompression melting led to initial flood basalts (Columbia River Flood Basalts, OR and the High Rock caldera complex, NV) and then to silicic eruptions along the hot spot track. Around 14-10 Ma, a transition from plume head to plume tail resulted in better aligned rhyolitic volcanic centers and calderas along the axis of the eastern Snake River Plain (Pierce et al., 1992; Coble and Mahood, 2016). Basaltic volcanism began shortly after the demise of rhyolitic volcanism at each center with flow ages ranging from thousands to several million years old (Armstrong et al., 1975).

Basaltic Volcanism on the Snake River Plain

Basaltic volcanism on the Snake River Plain has been called “plains style” volcanism as it has distinct flow characteristics, surface morphologies, and geochemistry compared to continental flood basalts and large Hawaiian-type shield volcanoes (Greeley, 1982; Christiansen and McCurry, 2008; Hughes et al., 2018). Clusters of tens to thousands of monogenetic low-shield volcanoes are a characteristic aspect of a basaltic plains region (Walker and Sigurdsson, 2000).

Presumably, development of low-shield volcanoes on the Snake River Plain begins with partial melting of the Yellowstone plume between 80 and 110 km depth (e.g., Leeman and Vitaliano, 1976; Bradshaw, 2012; Jean et al., 2013; Putirka et al., 2009; Jean et al., 2018). Magma ascends from that depth and eventually stagnates in the crust where fractional crystallization and incorporation of local partially melted country rock occurs. Stagnation depth is probably controlled by the strength of the crustal rocks, rather than density, to form the mid-crustal sill, inferred to be a complex network of individual bodies of magma that fractionate independently and represent single pulses of magma that feed individual monogenetic low-shield volcanoes (Potter et al., 2018; Potter et al., 2019). As the basaltic magmas crystallize and evolve, the reservoirs are continually fed by repeated influx of mafic magma before erupting (Leeman and Vitaliano, 1976; Leeman, 1982; Hanan et al., 2008; Potter et al., 2018).

Small volumes of magma (0.01-15 km^3), that have little substantial residence time in the crust, erupt from fissures or central vents over a time span of a few days to years to form large tube- and channel-fed lava fields some tens of kilometers across (Greeley, 1982; Geist et al., 2002; Walker and Sigurdsson, 2000; Hughes et al., 2002; Hughes et al., 2018). Small topographic shields typically less than 200 m high and ~15 km across mark the central vents. The polygenetic lava field grows as volcanoes accumulate on top of each other covering the distal flows but leaving the slightly steeper upper portion of the shields exposed. Eventually, these summits are also buried. The summit regions are typically marked by irregular pit craters filled with small lava lakes, shelly pahoehoe, ropy pahoehoe, and short spatter-fed flows. Lava lake overflow and “underflow” into tubes are important mechanism of shield growth (Greeley, 1982; Hughes et al., 1999; Hughes et al., 2018).

METHODS

Existing geologic maps (Malde et al., 1963; LaPoint, 1977; Bond et al., 1978; Othberg et al., 2012; Kuntz et al., 2018) were modified during field exploration and sampling (Fig. 2). Samples were collected around each shield from the distal flow margins, the flanks of the shield, and near the summit vents. Additionally, lava flow types (olivine-rich, intermediate, plagioclase-rich) were mapped. At Rocky Butte, strike and dip measurements were recorded for slabby ramparts along with flow descriptions (spatter, lava flow, spatter-

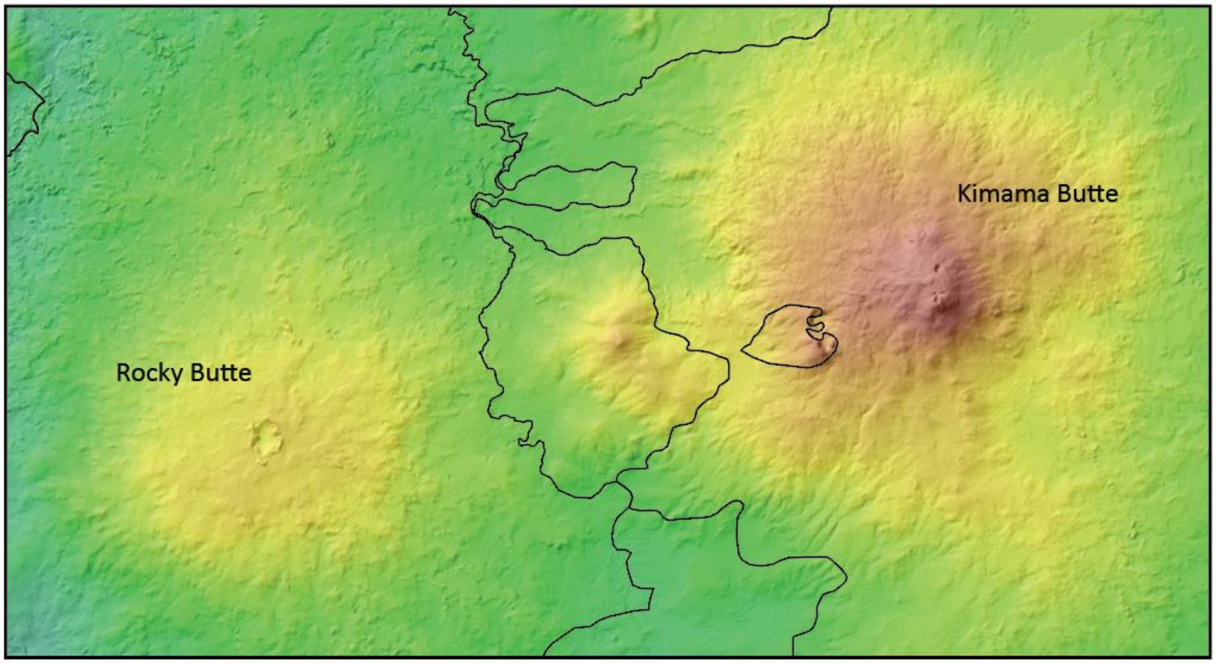

Figure 2. A colored shaded relief map showing the summit regions of Kimama Butte and Rocky Butte and parts of the lava fields. Lava from an older shield forms a kipuka just west of the Kimama Butte summit.

fed flow, etc.) at points around the rim and inside the lava lake. Sample locations and other field information were compiled on detailed geologic and topographic maps in ArcGIS using aerial photographs, and new digital elevation models derived photogrammetrically.

Whole rock major and trace element analyses were performed by x-ray fluorescence spectrometry and major element analysis of pre-eruptive phases (olivine, plagioclase, and spinel) by electron microprobe were performed at Brigham Young University. Inductively Coupled Plasma- Mass Spectrometry analyses of several samples were conducted commercially by ALS Global. Trace-element abundances in olivine, plagioclase, and spinel were analyzed by LA-ICP-MS at the University of Utah. Trace element data were processed at Brigham Young University using Iolite (Paton et al., 2011).

GEOLOGY OF KIMAMA BUTTE

Kimama Butte lavas erupted 87 ± 11 ka ($^{40}Ar/^{39}Ar$ weighted mean plateau age using 1.196 Ma for the age of the Alder Creek Rhyolite standard; Kuntz et al., 2018) and cover an area of about 250 km^2 (Fig. 2). From the main vent, ~10 km^3 of lava distributed in a broad low-profile shield 13 km in diameter and 240 m high (Fig. 1). Individual hummocky lava flows built on each other to create the broad shield. Tube-fed flows make up the medial and distal portions of the shield and extend as far as 20 km from the vent. Tumuli developed throughout the flow area. Thin deposits (< 2 m) of eolian sand and loess cover local portions of the shield.

Kimama Butte has a cap-like, steep-sided vent region on top of its typical shield profile (Fig. 1; Christiansen and Hurst, 2004). The main summit vent is marked by two adjoining sets of north-south trending ramparts instead of a central crater (about 150 m apart with a combined length of about 500 m). The ramparts are as high as 50 m (the southern ramparts being taller than the northern ramparts) and consist of inclined sheets of thin, weakly to moderately vesicular flows ranging from 3-10 cm thick. Thicker layers are about 1 m thick with slightly higher vesicularity but the same phenocryst percentages as the thinner accumulations. Some sheets of thin flows dip into the crater while others dip away from the crater. Shelly pahoehoe flows dominate the vent area. The ramparts typically contain greater than 30% phenocrysts with small glomerocrystic/ cumulate bombs about 2-3 cm in diameter scattered throughout. The bombs have large, almost radial, laths of plagioclase with smaller grains of olivine.

About 350 m north of the main vent area, collapse created a small pit crater 15 m deep and 150 m in diameter. The base of the southern wall of the crater is a 3-4 m thick, phenocryst-poor (3-15 vol% phenocrysts) massive basalt with increasing vesicularity up-section. Near the top of this unit several smaller 10-20 cm thick flows or flow lobes exist. Above these thinner flows, more massive phenocryst-rich flows (>30 vol% phenocrysts) extend for another 3-4 m. These are similar in composition and phenocryst percentage to the ramparts at the vent to the south but lack the small plagioclase bombs. The top meter of the pit crater wall consists of thinner flows.

GEOLOGY OF ROCKY BUTTE

In contrast, Rocky Butte has a broad topographic shield 36 km across that rises 100 m to a summit with less than 1° slopes (Fig. 1). The shield consists of approximately 15 km^3 of lava that erupted 95 ± 10 ka ($^{40}Ar/^{39}Ar$ weighted mean plateau age; using an age of 27.92 for the Taylor Creek Rhyolite; Tauxe et al., 2004). Lava emplaced through tube- and channel-fed flows filled a former canyon of the Snake River and formed the wide shield (Fig. 2). Vesicular pahoehoe lava with multiple tumuli (both as cracked ridges and flat-topped plateaus with inflation pits and fissured margins) form hummocky flows indicative of moderate effusion rates (e.g. Self, 1998). The flows extend about 40 km from the vent to the southwest as far as the city of Twin Falls where they are found on the north side of the Snake River Canyon.

The summit of Rocky Butte is marked by a shallow crater about 25 m deep and slightly elongated to the north and south (about 970 m by 680 m). The crater is almost completely surrounded by a narrow ridge (100-140 m wide at ~1375 m elevation) with undulating topography of mounds (1-8 m tall) and intervening lows. The high mounds on the crater rim are discontinuous vesicular blocks that contain sequences of massive lava flows (~1 m thick). The outer blocks dip away from the crater at 30°-50°. At most places along the rim, another set of discontinuous blocks runs parallel to the outermost blocks. These inner sections are a few meters away from the outer sections and dip in the opposite direction, that is into the crater.

Several meters down slope into the crater (~1365 m elevation), there is a bench of randomly oriented blocks. Large mounds (~4 m tall) and smaller broken up blocks set at different angles are present on the floor of the crater. The lowest section of the crater floor (~1349 m elevation) is in the northwestern part of the crater. Thin flows and shelly and rope-like pahoehoe surfaces are present in this region. Regardless of their position relative the vent, the basalt at Rocky Butte has small phenocrysts of olivine and plagioclase set in a dark, fine-grained vesicular to diktytaxitic matrix.

RESULTS

Whole rock compositions of the olivine tholeiites range in TiO_2 concentrations from

2.6-4.5 wt% for Kimama Butte and 2.6-4.3 wt% for Rocky Butte. These ranges can be related to magma evolution suggesting eruptive products with compositions probably controlled by fractional crystallization. The composition of lavas from Kimama and Rocky Butte are very similar. MgO, Al_2O_3, and Fe_2O_3 show the most difference between the two volcanoes with Rocky Butte basalts having higher MgO and lower Al_2O_3 at a given TiO_2 content. Trace element concentrations are likewise similar for the two volcanoes. Ni and Cr, however, stand out just like MgO and Al_2O_3 in that they are systematically higher in Rocky Butte lavas than in those from Kimama Butte. Otherwise, the concentrations of trace elements follow similar trends with more samples falling in the more chemically primitive end of the spectrum and fewer samples extending to the evolved side. At either volcano, there is no correlation between chemical composition and distance from the vent.

Compositions of the pre-eruptive phenocrysts, olivine and plagioclase, are similar across both shields but show variation with evolution. The centers, or 'cores', of olivine in the more primitive samples are more Mg-rich (Fo_{80-72}) than those in the evolved rocks (Fo_{65-55}). In both cases, thin Fe-rich rims are often present. Ni, Cr, and Al concentrations are higher in the more primitive samples than in the evolved. Plagioclase 'cores' are similarly more calcic in the more primitive flows (An_{78-68}) than in the evolved ones (An_{65-52}). Plagioclase in the primitive rocks typically have less Ti, Ba, and Fe and more Mg than evolved samples.

Like other olivine-tholeiites on the Snake River Plain, the fO_2 and fH_2O were probably low with fO_2 at -2△QFM and 0.1 wt% H_2O (e.g. Whitaker et al., 2007; Bradshaw, 2012). Pressure estimated from MELTS models (Gualda et al., 2012; Gualda and Ghiorso, 2015) seems to be around 3 kbar correlating with fractionation at 10 km depth. Temperatures (1226-1147°C vs 1251-1145°C) and melt viscosities (19-8 Pa·s vs 14-7 Pa·s) overlap at both Kimama and Rocky Butte (Putirka, 2008; Shaw, 1972).

DISCUSSION

Volcanic landforms, whether on Earth or elsewhere, are the result of complex interactions of many factors (e.g., Wilson, 2009; Wilson and Head, 2018). On the Snake River Plain, variations in these aspects produced two adjacent morphologically different shield volcanoes that erupted within a relatively short time of each other. Whole rock and mineral compositions, eruptive temperatures, and melt viscosity overlap at Kimama Butte and Rocky Butte and thus are likely not main controls on shield morphology. Similarly, magma evolution is alike at the two shields. Processes that may differ at the two shields include magma viscosity, phenocryst abundance, and eruption style.

Phenocryst Content

At Kimama Butte, phenocryst abundance ranges from 3-39 vol% (Fig. 3). Three main varieties of basalt are defined by phenocryst content. The first type, phenocryst-poor basalt, contains less than 15 vol% olivine and plagioclase. The second variety, phenocryst-

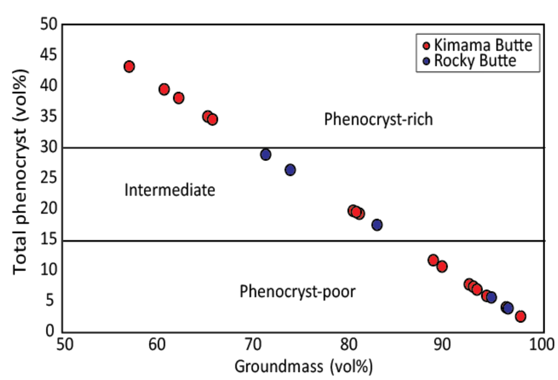

Figure 3. Distribution of Kimama Butte lavas in the three phenocryst varieties. The range in phenocryst abundance at Rocky Butte does not extend as high as Kimama Butte.

rich basalts, have greater than 30 vol% phenocrysts. The third type of lavas at Kimama Butte are intermediate with plagioclase and olivine comprising an average of 19 vol%.

The phenocryst-poor basalts are the most widespread variety found in distal flows, on the flanks of the shield, and the base of the pit crater walls. Intermediate type lavas occur only on the flanks of the shield within 5-9 km of the summit. Phenocryst-rich basalts are found within 4 km of the summit. This distribution of phenocryst percentages suggests that phenocryst-poor lavas erupted first from Kimama Butte, as found at other Snake River Plain shields (Casper, 1999; Hughes et al., 2002; Brady, 2005).

Variation in crystal content at Rocky Butte is less pronounced then at Kimama Butte (4-29 vol%; Fig. 3). The average percent of phenocrysts at Rocky Butte matches most closely with that of the intermediate lavas of Kimama Butte. Phenocryst-rich lavas, like those found near the vent at Kimama Butte, are not present in distal flows or at Rocky Butte. Additionally, at Rocky Butte, no correlation has been found between position on the shield and phenocryst amount. At either volcano, there is no clear relationship between phenocryst content and lava composition.

Magma Viscosity

The steep summit areas found on some shield volcanoes in the Snake River Plain, like Kimama Butte, may be due to an increase in lava crystallinity and hence viscosity near the vent (Sakimoto et al., 2003). Lavas with a higher phenocryst content should have higher viscosities and form shorter thicker flows given similar eruption rates, compositions, and temperatures. Magma viscosities (Fig. 4) calculated with the Einstein-Roscoe equation (Marsh, 1981) and phenocryst proportions overlap at Kimama Butte (14 to 158 Pa·s) and Rocky Butte (8 to 75 log Pa·s), but Kimama Butte viscosities extend ~80 Pa·s higher than Rocky Butte.

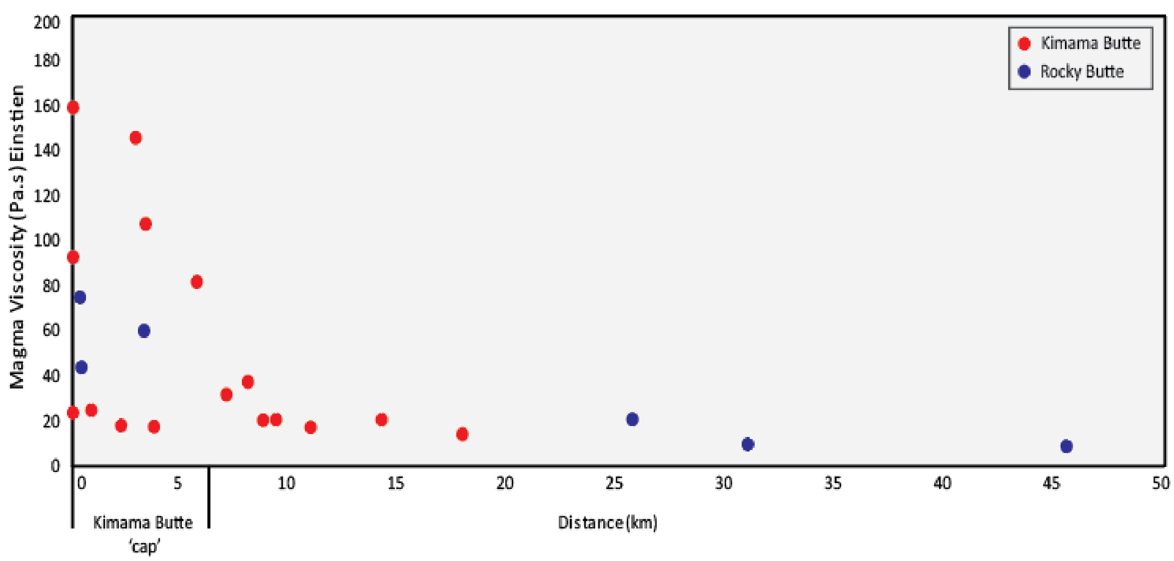

Figure 4. Calculated viscosity as a function of distance from summit at the two volcanoes. Magma viscosities were determined using the Einstein-Roscoe equation (Marsh, 1981). Phenocryst percentages were determined by point counting. Magma viscosities at the summit of Kimama Butte are higher and more variable than at Rocky Butte. Some of the low viscosities near the vent at Kimama Butte are from the base of the pit crater and thus represent earlier flows.

Crystallinity and viscosity are significantly higher at the summit of Kimama Butte (up to 158 Pa·s with 39 vol% phenocrysts) than on the flanks (as low as 14 Pa·s with 3 vol% phenocrysts). The crystallinity and viscosities of near-vent lavas at Rocky Butte (43-75 Pa·s with 26-29 vol% phenocrysts) are much less than at the summit of Kimama Butte (Fig. 4). In contrast, the distal flows from Rocky Butte and Kimama Butte have similar phenocryst proportions and low viscosities (<20 Pa·s). Thus, it appears that lava viscosity and phenocryst content may play a role in development of the shape of these two volcanoes.

Eruption Style

Another factor to consider in the creation of different shield morphologies is differences in eruptive style both between shields and with time at a single shield volcano. Brady (2005) suggested that a viscosity related change in eruption style at Quaking Aspen Butte, another shield volcano on the eastern Snake River Plain, may have focused the fissure to a pipe-like vent. The centralized fountaining then would have formed a steep cap. An interpretation of field observations at these two shields suggest a similar event could have happened at Kimama Butte but not Rocky Butte.

The shallow vent crater at Rocky Butte likely developed as a large lava blister that inflated, collapsed and was then filled by a lava lake (Fig. 5). The variably tilted discontinuous vesicular blocks found around the rim and within the crater are the main evidence for a swelling or bulging blister as the tilting occurred after lava emplacement. Inflation would cause extensional fractures along the edges of the uplift. As swelling subsided and the feature deflated or collapsed, the inward dipping ramparts formed.

After the crater collapsed, a lava lake developed at Rocky Butte. The benches stepping down into the crater are interpreted as margins of a sequentially draining lava lake and the lowest section of the crater floor is taken as the last area of lava lake retreat. Small fountains along the lake margins formed little spatter deposits seen as large mounds on the crater floor. Moderate to high accumulation rates resulted in welded spatter that flowed short distances (Head and Wilson, 1989).

In contrast, a topographic break occurs at Kimama Butte ~7 km from the vent where the broad gently sloping shield steepens. The phenocryst-rich basalt variety is only present at the cap within 4 km of the vent. Short flows, interpreted as spatter-fed because of vesicle shapes and trains, make up the high ramparts near the vent region. The calculated viscosity of these spatter fed flows are as much as 8 times higher than the earlier tube and overflow lavas (14 vs. 158 Pa·s).

The high ramparts at Kimama Butte likely formed by moderate to high rates of spatter accumulation during prolonged fountaining (Fig. 5; Head and Wilson, 1989). The pit crater north of the spatter ramparts formed after fountaining ceased as it exhibits the succession of lava found around Kimama Butte, yet no new lava flowed over the rim into the crater.

The broad topographic shields at Rocky and Kimama Butte were formed similarly from initial fountaining followed by lava lake overflow combined with the buildup of tube- and channel-fed flows. After initial shield development occurred, the eruptive activity diverged at the two shields when late fountaining at Kimama Butte added several meters of height to the shield that is missing from Rocky Butte where no late fountaining occurred (Fig. 5).

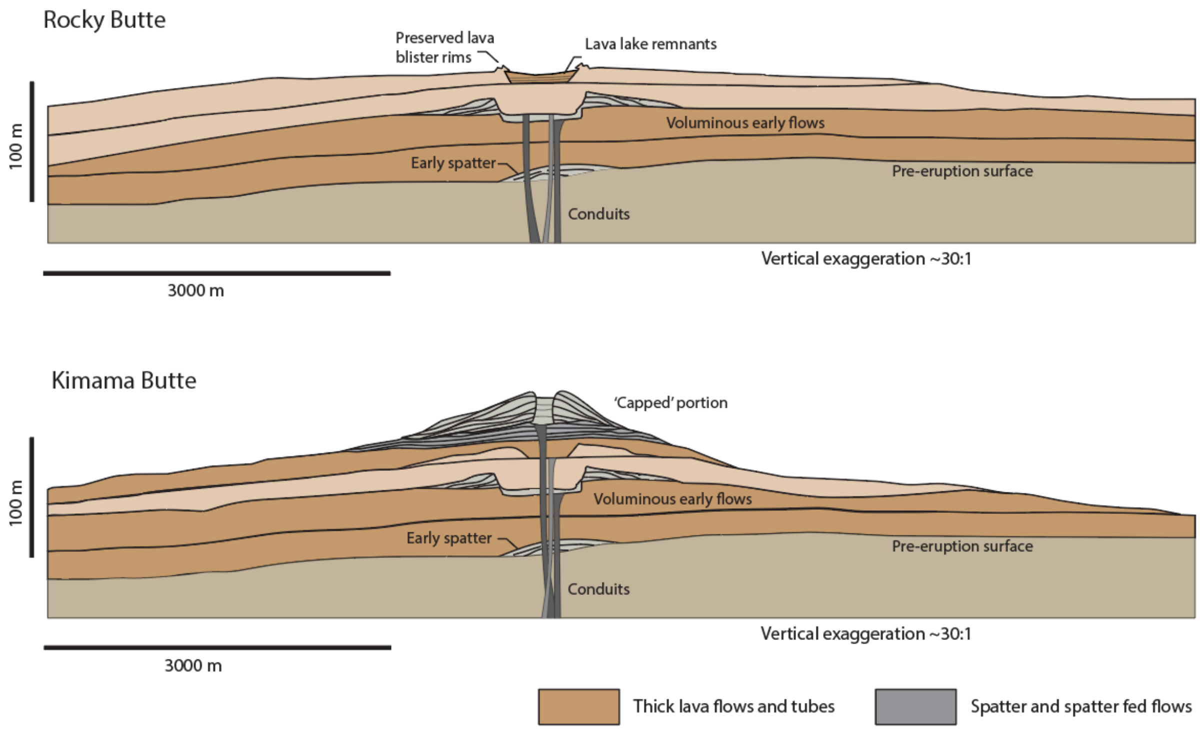

Figure 5. Schematic cross sections of Kimama Butte and Rocky Butte. The vent crater at Rocky Butte developed as a large lava blister that inflated and then collapsed forming a crater in which a lava lake developed. In contrast, high spatter mounds flank the main summit crater at Kimama Butte.

CONCLUSIONS

Understanding Kimama Butte and Rocky Butte, two shield volcanoes on the eastern Snake River Plain of Idaho, enlarges the arsenal of methods to determine characteristics of volcanoes throughout the solar system that we are not able to sample or study insitu. Rocky Butte is a broad low shield (36 km across with ~1° slopes) with a summit crater; Kimama Butte is higher and has a steep-summit cap that lacks a central crater (18 km across and 210 m high). The vent crater at Rocky Butte developed as a large lava blister that inflated and then collapsed forming a crater in which a lava lake developed. Little spatter accumulated there. In contrast, high spatter mounds and spatter fed flows flank the main summit crater at Kimama Butte.

Major and trace-element variation as well as mineral assemblages and compositions are similar at the two shields. Major and trace element models (including MELTS) suggest that lavas from both shields appear to have evolved by fractional crystallization at 3 kbar (~10 m depth). Eruptive temperatures overlap at Kimama Butte and Rocky Butte. The similarity of these factors at the two volcanoes suggests that they are probably not important controls on shield volcano morphology. Thus, it would be difficult to use shield profiles to speculate about magma composition differences or differences in the degree of magma evolution for similar shield volcanoes on other planetary bodies as suggested by Hughes and Sakimoto (2002) and Sakimoto et al. (2002).

Shield morphology does seem to be related to phenocryst content (and therefore magma viscosity) and eruption style. Lavas near the summit at Kimama Butte contain more phenocrysts and have viscosities double the value of lavas near the vent at Rocky Butte. Additionally, the high magma viscosities (up to 158 Pa·s with 39 vol% phenocrysts) at Kimama Butte are confined to the steep summit cap of the shield.

A reasonable history of shield growth at Kimama Butte and Rocky Butte involves a similar initial period of fountaining, lava lake overflow, and tube- and channel- fed flows. Late fountaining at Kimama Butte deposited the phenocryst-rich, higher viscosity lavas and high spatter ramparts that form the cap. Rocky Butte did not experience an episode of late fountaining, so no steep cap developed there.

References

Armstrong, R., Leeman, W. P., and Malde, H. E., 1975, K--Ar dating quaternary and Neogene volcanic rocks of the Snake River Plain, Idaho: Am. J. Sci.;(United States), v. 275, no. 3.

Bond, J., Kauffman, J., Miller, D., and Venkatakrishnan, R., 1978, Geologic Map of Idaho: Moscow: Idaho, Idaho Department of Lands, Bureau of Mines and Geology, scale, v. 1, no. 500,000, p. 1.

Bradshaw, R. W., 2012, Mineral chemistry of basalts recovered from Hotspot Snake River Scientific Drilling Project, Idaho: source and crystallization characteristics: Brigham Young University.

Brady, S. M., 2005, Controls on basaltic shield morphology, eastern Snake River Plain, Idaho: A textural and geochemical study of Table Legs Butte and Quaking Aspen Butte: Idaho State University.

Casper, J., 1999, The volcanic evolution of Circular Butte: Idaho State University.

Christiansen, E. H., and Hurst, M., 2004, Vent Geology of Low-Shield Volcanoes from the Central Snake River Plain, Idaho: Lessons for Mars and the Moon, *in* Proceedings Lunar and Planetary Science Conference, v. 35.

Christiansen, E. H., and McCurry, M., 2008, Contrasting origins of Cenozoic silicic volcanic rocks from the western Cordillera of the United States: Bulletin of Volcanology, v. 70, no. 3, p. 251-267.

Christiansen, R. L., Foulger, G., and Evans, J. R., 2002, Upper-mantle origin of the Yellowstone hotspot: Geological Society of America Bulletin, v. 114, no. 10, p. 1245-1256.

Coble, M. A., and Mahood, G. A., 2016, Geology of the High Rock caldera complex, northwest Nevada, and implications for intense rhyolitic volcanism associated with flood basalt magmatism and the initiation of the Snake River Plain–Yellowstone trend: Geosphere, v. 12, no. 1, p. 58-113.

Colón, D. P., Bindeman, I. N., and Gerya, T. V., 2018, Thermomechanical modeling of the formation of a multilevel, crustal-scale magmatic system by the Yellowstone plume: Geophysical Research Letters, v. 45, no. 9, p. 3873-3879.

Foulger, G. R., Christiansen, R. L., and Anderson, D. L., 2015, The Yellowstone "hot spot" track results from migrating basin-range extension: The Interdisciplinary Earth: A Volume in Honor of Don L. Anderson: Geological Society of America Special Paper, v. 514, p. 215-238.

Geist, D. J., Sims, E. N., Hughes, S. S., and McCurry, M., 2002, Open-system evolution of a single episode of Snake River Plain magmatism: Geology, hydrogeology, and environmental remediation: Idaho National Engineering and Environmental Laboratory, eastern Snake River Plain, Idaho, v. 353, p. 193.

Greeley, R., 1982, The style of basaltic volcanism in the eastern Snake River Plain, Idaho, Cenozoic geology of Idaho: Idaho Bureau of Mines and Geology Bulletin, v. 26, p. 407-421.

Greeley, R., and Spudis, P. D., 1981, Volcanism on mars: Reviews of Geophysics, v. 19, no. 1, p. 13-41.

Gualda, G. A., and Ghiorso, M. S., 2015, MELTS _ E xcel: AM icrosoft E xcel-based MELTS interface for research and teaching of magma properties and evolution: Geochemistry, Geophysics, Geosystems, v. 16, no. 1, p. 315-324.

Gualda, G. A., Ghiorso, M. S., Lemons, R. V., and Carley, T. L., 2012, Rhyolite-MELTS: a modified calibration of MELTS optimized for silica-rich, fluid-bearing magmatic systems: Journal of Petrology, v. 53, no. 5, p. 875-890.

Guest, J. E., Bulmer, M. H., Aubele, J., Beratan, K., Greeley, R., Head, J. W., Michaels, G., Weitz, C., and Wiles, C., 1992, Small volcanic edifices and volcanism in the plains of Venus: Journal of Geophysical Research: Planets, v. 97, no. E10, p. 15949-15966.

Hanan, B. B., Shervais, J. W., & Vetter, S. K., 2008, Yellowstone plume–continental lithosphere interaction beneath the Snake River Plain: Geology, v. 36, p. 51-54.

Hauber, E., Bleacher, J., Gwinner, K., Williams, D., & Greeley, R., 2009, The topography and morphology of low shields and associated landforms of plains volcanism in the Tharsis region of Mars: Journal of Volcanology and Geothermal Research, v. 185, p. 69-95.

Head, J. W., and Gifford, A., 1980, Lunar mare domes: Classification and modes of origin: The moon and the planets, v. 22, no. 2, p. 235-258.

Head, J. W., and Wilson, L., 1989, Basaltic pyroclastic eruptions: influence of gas-release patterns and volume fluxes on fountain structure, and the formation of cinder cones, spatter cones, rootless flows, lava ponds and lava flows: Journal of Volcanology and Geothermal Research, v. 37, p. 261-271.

Head, J. W., and Wilson, L., 1992, Lunar mare volcanism: Stratigraphy, eruption conditions, and the evolution of secondary crusts: Geochimica et Cosmochimica Acta, v. 56, no. 6, p. 2155-2175.

Henderson, A. O., 2015, Low-shield volcanism: a comparison of volcanoes on Syria Planum, Mars and Snake River Plain, Idaho: Brigham Young University.

Hughes, S. S., Smith, R. P., Hackett, W. R., and Anderson, S. R., 1999, Mafic volcanism and environmental geology of

the eastern Snake River Plain, Idaho: Guidebook to the geology of eastern Idaho, p. 143-168.
Hughes, S. S., 2001, Mafic volcanism on the Eastern Snake River Plain: Petrologic evaluation of a terrestrial analogue for planetary bodies, *in* Proceedings Lunar and Planetary Science Conference, v. 32.
Hughes, S. S., Wetmore, P. H., and Casper, J. L., 2002, Evolution of Quaternary tholeiitic basalt eruptive centers on the eastern Snake River Plain, Idaho: Tectonic and Magmatic Evolution of the Snake River Plain Volcanic Province: Idaho Geological Survey Bulletin, v. 30, p. 363-385.
Hughes, S., Sakimoto, S., Gregg, T., Chadwick, D., Brady, S., Farley, M., Holmes, A., Semple, A., and Weren, S., 2004, Topographic Evidence for Eruptive Style Changes and Magma Evolution of Small Plains-style Volcanoes on Earth and Mars.
Hughes, S. S., Nawotniak, S. E. K., Sears, D. W., Borg, C., Garry, W. B., Christiansen, E. H., Haberle, C. W., Lim, D. S., and Heldmann, J. L., 2018, Phreatic explosions during basaltic fissure eruptions: Kings Bowl lava field, Snake River Plain, USA: Journal of Volcanology and Geothermal Research, v. 351, p. 89-104.
Hughes, S. S., Haberle, C. W., Kobs Nawotniak, S. E., Sehlke, A., Garry, W. B., Elphic, R. C., Payler, S. J., Stevens, A. H., Cockell, C. S., and Brady, A. L., 2019, Basaltic terrains in Idaho and Hawai ʻi as planetary analogs for Mars geology and astrobiology: Astrobiology, v. 19, no. 3, p. 260-283.
Jean, M. M., Shervais, J. W., Champion, D. E., and Vetter, S. K., 2013, Geochemical and paleomagnetic variations in basalts from the Wendell Regional Aquifer Systems Analysis (RASA) drill core: Evidence for magma recharge and assimilation–fractional crystallization from the central Snake River Plain, Idaho: Geosphere, v. 9, no. 5, p. 1319-1335.
Jean, M. M., Christiansen, E. H., Champion, D. E., Vetter, S. K., Phillips, W. M., Schuth, S., and Shervais, J. W., 2018, Caldera life-cycles of the Yellowstone hotspot track: death and rebirth of the Heise Caldera: Journal of Petrology, v. 59, no. 8, p. 1643-1670.
Kuntz, M. A., Champion, D. E., Turrin, B. R., Gans, P. B., Covington, H. R., and VanSistine, D. P., 2018, Geologic map of the north half of the Lake Walcott 30'× 60'quadrangle, Idaho: US Geological Survey, 2329-132X.
LaPoint, P. J., 1977, Preliminary photogeologic map of the eastern Snake River Plain, Idaho.
Leeman, W., and Vitaliano, C., 1976, Petrology of McKinney Basalt, Snake River Plain, Idaho: Geological Society of America Bulletin, v. 87, no. 12, p. 1777-1792.
Leeman, W. P., 1982a, Development of the Snake River Plain-Yellowstone Plateau province, Idaho and Wyoming: an overview and petrologic model: Cenozoic geology of Idaho: Idaho Bureau of Mines and Geology Bulletin, v. 26, p. 155-177.
Malde, H. E., Powers, H. A., and Marshall, C. H., 1963, Reconnaissance geologic map of west-central Snake River Plain, Idaho.
Marsh, B., 1981, On the crystallinity, probability of occurrence, and rheology of lava and magma:
Hughes, S. S., and Sakimoto, S. E. H., 2002, Plains volcanism in the eastern Snake River Plain: Quantitative Measurements of petrologic contributions to topography with comparisons to Mars, *in* Proceedings Denver Annual Meeting 2002.

Contributions to Mineralogy and Petrology, v. 78, no. 1, p. 85-98.
McQuarrie, N., and Rodgers, D. W., 1998, Subsidence of a volcanic basin by flexure and lower crustal flow: The eastern Snake River Plain, Idaho: Tectonics, v. 17, no. 2, p. 203-220.
Othberg, K. L., Kauffman, J. D., Gillerman, V. S., and Garwood, D. L., 2012, Geologic Map of the Twin Falls 30 x 60 Minute Quadrangle, Idaho, Idaho Geological Survey, University of Idaho.
Paton, C., Hellstrom, J., Paul, B., Woodhead, J., and Hergt, J., 2011, Iolite: Freeware for the visualisation and processing of mass spectrometric data: Journal of Analytical Atomic Spectrometry, v. 26, no. 12, p. 2508-2518.
Perfit, M. R., and Davidson, J. P., 2000, Plate tectonics and volcanism: Encyclopedia of Volcanoes, p. 89-113.
Pierce, K. L., Morgan, L. A., and Link, P., 1992, The track of the Yellowstone hot spot: Volcanism, faulting, and uplift: Regional geology of eastern Idaho and western Wyoming: Geological Society of America Memoir, v. 179, no. 322, p. 1-53.
Potter, K. E., Shervais, J. W., Christiansen, E. H., and Vetter, S. K., 2018, Evidence for cyclical fractional crystallization, recharge, and assimilation in basalts of the Kimama drill core, central Snake River Plain, Idaho: 5.5-million-years of petrogenesis in a mid-crustal sill complex: Frontiers in Earth Science, v. 6, p. 10.
Potter, K. E., Champion, D. E., Duncan, R. A., and Shervais, J. W., 2019, Volcanic stratigraphy and age model of the Kimama deep borehole (Project Hotspot): Evidence for 5.8 million years of continuous basalt volcanism, central Snake River Plain, Idaho: Geosphere, v. 15, no. 3, p. 736-758.
Putirka, K. D., 2008, Thermometers and barometers for volcanic systems: Reviews in mineralogy and geochemistry, v. 69, no. 1, p. 61-120.
Putirka, K. D., Kuntz, M. A., Unruh, D. M., and Vaid, N., 2009, Magma evolution and ascent at the Craters of the Moon and neighboring volcanic fields, southern Idaho, USA: implications for the evolution of polygenetic and monogenetic volcanic fields: Journal of Petrology, v. 50, no. 9, p. 1639-1665.
Sakimoto, S., Gregg, T., Hughes, S., and Chadwick, J., 2003, Re-assessing plains-style volcanism on Mars, *in* Proceedings Sixth International Conference on Mars, Abstract 3197.
Sakimoto, S., Mitchell, D., Riedel, S., and Taylor, K., 2002, Small Shield Volcanoes on Mars: Global Geometric Properties and Model Implications for Regional Varations in Eruptive Styles, *in* Proceedings Lunar and Planetary Science Conference, v. 33.
Tauxe, L., Luskin, C., Selkin, P., Gans, P., and Calvert, A., 2004, Paleomagnetic results from the Snake River Plain: Contribution to the time-averaged field global database: Geochemistry, Geophysics, Geosystems, v. 5, no. 8.

Walker, G. P., and Sigurdsson, H., 2000, Basaltic volcanoes and volcanic systems: Encyclopedia of volcanoes, p. 283-289.

Whitaker, M., Nekvasil, H., Lindsley, D., and Difrancesco, N., 2007, The role of pressure in producing compositional diversity in intraplate basaltic magmas: Journal of Petrology, v. 48, no. 2, p. 365-393.

Wilson, L., 2009, Volcanism in the solar system: Nature Geoscience, v. 2, no. 6, p. 389-397.

Wilson, L., and Head, J., 2018, Controls on lunar basaltic volcanic eruption structure and morphology: Gas release patterns in sequential eruption phases: Geophysical Research Letters, v. 45, no. 12, p. 5852-5859.